ENHANCED MECHANICAL SEAL PERFORMANCE THROUGH PROPER SELECTION AND APPLICATION OF ENLARGED-BORE SEAL CHAMBERS

by

William V. Adams

Vice President, Engineering, Research and Quality Assurance

Richard H. Robinson

Director, Research and Development

James S. Budrow

Engineering Specialist

Durametallic Corporation

Kalamazoo, Michigan

William V. Adams received a degree in Mechanical Engineering from Western Michigan University (1967). He is currently Vice President of Engineering, Research and Quality Assurance for the Durametallic Corporation. During Mr. Adam's 25 years with the company, he has held assignments as a Research Engineer, Assistant Manager of Engineering, Chief Design Engineer and Director of Engineering. In 1984, he was named Vice President of Engineering and Research and in 1989 Quality Assurance was added to his responsibilities.

Professionally, Mr. Adams has served on the ASME B73 Chemical Pump Standards Committee for the past five years. He is past Chairman of the Seals Technical Committee of STLE and has served as their Educational Committee Chairman and Vice Chairman of their Standards Committee. Currently, he is Chairman of their WG-3 Emissions Task Force and is a member of the API 682 Seal Standards Committee.

Richard Robinson is Director of Research and Development. He joined Durametallic in 1987 as Director of Engineering Operations after serving in design, product development, and engineering management positions with an industrial equipment firm. He received a B.S.M.E. degree from Purdue University and is a member of ASME and STLE.

James Budrow is an Engineering Specialist in the Research and Development Department. He has made major contributions in the areas of bellows seals, split seals, dry running seals, and abrasive slurry sealing development and has written numerous articles on these subjects. He received a B.S.M.E. degree from Western Michigan University and is a member of ASME.

ABSTRACT

Recent studies of enlarged-bore seal chambers document the influence of chamber design on seal performance. The studies utilize laser doppler velocimetry (LDV), high speed videography, and computational fluid dynamics (CFD) to model seal chamber characteristics. Off-design pump operation and dry-running conditions are studied. An erosion index value (EIV) is proposed as a means to predict and avoid erosion problems. The effects of devices protruding into the seal chamber on particle flow are reported. Guidelines are provided to assist in selecting seal chamber designs and environmental controls for specific applications.

INTRODUCTION

Industry demand for longer mean time between planned maintenance (MTBPM) of pumps has resulted in increased interest in the factors affecting the life of mechanical seals. One key factor is the environment or envelope surrounding the seal, the seal chamber. Worldwide pump standards have been updated to permit the use of optional enlarged, seal-only chambers. As a result, research on seal chambers has increased in recent years to extend the MTBPM of rotary equipment and to provide a more positive seal for controlling emissions to our environment [1]. The results of the current research allow the users and designers of mechanical seals to more accurately predict seal performance, understand effects of seal chamber design, and thereby take full advantage of enlarged-bore seal chambers.

Historically, seal users and manufacturers have been handicapped by having to adapt the mechanical seal to a cavity designed for compression packing, Figure 1. Axial and radial dimensions of this cavity were initially established for packing and a lantern ring. The stuffing box pressure was also minimized to reduce loads on the packing and minimize leakage to the atmosphere.

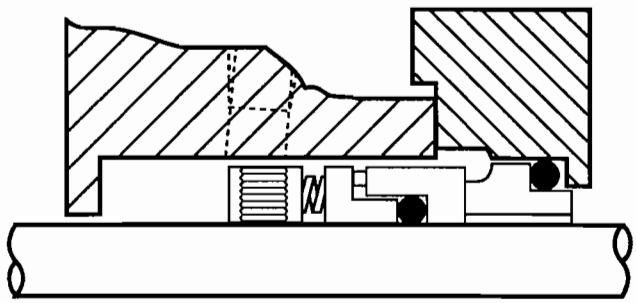

Figure 1. Mechanical Seal Installed in a Conventional Pump Stuffing Box.

In the past decade, industry has been moving to standardize on chambers designed for mechanical seals only. ANSI [2], API [3], DIN [4], and ISO [5] all have, or are now working on, enlarged bore seal chamber standards aimed at increasing MTBPM by enhancing the space available and the environment for the mechanical seal (Figure 2). Some specific benefits that have been noted by these changes in industrial standards include:

- Greater axial and radial space to adapt desired seal arrangements and geometries. Room is available for larger cross section parts and dual seal arrangements.
- Improved heat transfer in the seal environment.
- Automatic venting of gases from the seal chamber prior to startup.
- Improved environments for handling off-design pump operation.
- Better environment for handling low boiling point margin fluids.
- Optimized environment for slurry seals.

While recent changes to seal chamber designs have been dramatic, it is obvious that greater benefits can be realized by a more thorough analysis of the factors affecting seal performance under various environmental conditions. For instance, erosion problems have been reported in some field installations of pumps equipped with enlarged seal chambers (Figure 3). Surveys conducted by the Erosion Task Group of the ASME/ANSI B73 Chemical Pump Standards Committee indicate that erosion problems have been encountered in approximately one percent of the more than 10,000 enlarged seal chambers installed to date. To achieve the cost benefits of longer MTBPM, the causes of erosion need to be identified. Also, information is needed on how enlarged seal chambers handle off-design pump operation, dry running, and air ingestion.

To achieve this goal, a five year study was initiated. The initial work regarding the dissipation of seal generated heat was reported by Davison [6]. Continuing research was aimed at gaining a better understanding of the interaction between seals, seal chambers, and pumps, taking full advantage of new analytical tools and test methods. This research led to the development of new predictive formulas and application guides proposed that can be used by industry to extend rotary equipment MTBPM.

TEST EQUIPMENT AND METHODS

Testing was conducted on an acrylic pump having internal dimensions which duplicated a standard 2 × 1-10 ANSI B73.1 pump. This helped to ensure that the test results would be based on actual pump dynamics (Figure 4). The clear acrylic allowed visualization through the pump casing and various seal chamber arrangements with laser doppler velocimetry (LDV) and high speed videography. Fluid flow, particle flow, gas entrapment, and cavitation throughout the pump and seal chamber were clearly observed with this arrangement.

The basic test circuit used in all tests is shown in Figure 5. It consists of the acrylic pump, seal chambers of various designs, valves, product reservoir, and temperature and pressure indicators as shown. All tests were conducted with the seal chamber dead ended, per API Flush Plan 02. The makeup tank is open to atmosphere and provides approximately 4.0 ft (1.2 m) of static head on the suction side of the pump. Variable speed and fixed speed 10 horsepower motors were used so that operation from 800 to 3500 rpm could be studied. A 1.875 in metal bellows seal was used in all tests so that comparative results on the effects of various seal chambers and impeller designs could be studied.

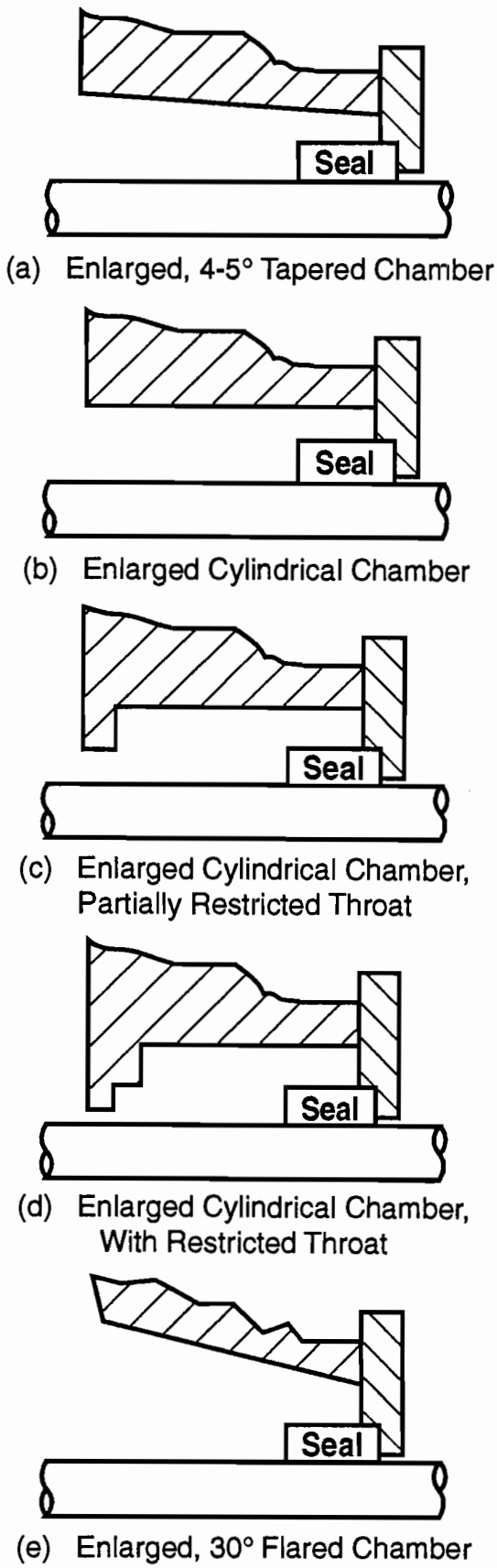

Figure 2. Mechanical Seal Installed in Optional Enlarged Seal Chambers.

A summation of radial and axial velocities within the seal chamber revealed that in open, enlarged cylindrical and tapered-bore seal chambers, the particles follow a helical path as they flow toward the gland face in a region close to the chamber bore and return toward the open throat in a region close to the rotating shaft (Figure 7). Moreover, a constant fluid exchange occurs between the chamber and the open throat.

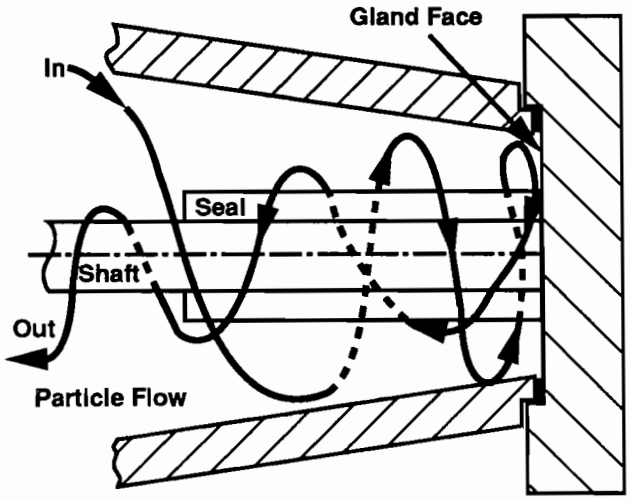

Figure 7. Particle Flow Path in Enlarged Seal Chamber.

The magnitudes of the flow velocities shown in Table 1 and the fluid pressure in the seal chamber are highly dependent on the chamber inlet flow conditions behind the impeller. Many of these velocities exceeded the shaft speed of 14.7 ft/sec (4.5 m/s). In some cases, the average flow velocities approached the velocity of the impeller at the exposed seal chamber opening. For a particular pump and rotational speed, the flow condition at the chamber inlet depends on the type of impeller, the inlet throat size, and the existence and size of impeller balance holes or back pumpout vanes. These also have a significant effect on the accumulation and flow of gases and solids within the seal chamber.

Table 1. Summary of LDV Test Results.

Chamber	Ref.	Throat Restriction	Balance Holes	Average Flow Speed ft/sec	m/s	Turbulence Intensity, %Max.
Enlarged 4° Tapered	Fig. 2 (a)	No	Yes	27.9	8.5	22
Enlarged 4° Tapered	Fig.2 (a)	No	No	6.6	2.0	9
Enlarged 4° Tapered	Fig. 8	Partial*	Yes	16.4	5.0	14
Enlarged Cylindrical	Fig. 2 (c)	Partial*	Yes	16.4	5.0	17
Enlarged 30 to 45° Flared	Fig. 2 (e)	No	Yes	26.9	8.2	24
Enlarged 30 to 45° Flared	Fig. 2 (e)	No	No	13.1	4.0	12

1.875 in. (47.6 mm) metal bellows mechanical seal
ANSI Pump, 10 in. (254 mm) impeller, 1800 rpm
* 2.909 inch (73.9 mm) diameter opening

The largest velocities were measured when the flow through the chamber was at a maximum. As can be seen in Table 1, the higher velocities were generated with enlarged cylindrical bore, four degree tapered bore, and 30 degree flared bore chambers all with balance holes in the impeller. Tests in the lab plus field experience reveal that high velocities are also achieved when the enlarged seal chamber bore significantly exposes the back pump-out vanes to the chamber, which is often the case.

Velocities were reduced when a partial throat restriction was used (Figure 8), blocking the effect of the impeller. By reducing the inlet throat diameter for the tapered chamber from 3.94 in to 2.91 in (100.1 mm to 73.9 mm), as shown in Figure 8, the average flow velocities dropped from 27.9 to 16.4 ft/sec (8.5 to 5.0 m/s). The smaller inlet restricts the mass flow into the tapered chamber and reduces the amount of energy imparted to the fluid by the impeller.

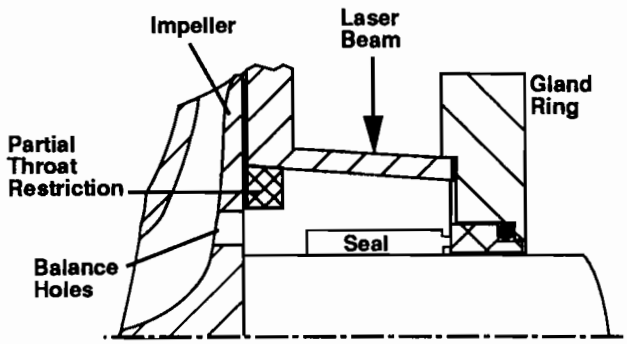

Figure 8. Enlarged Tapered Seal Chamber with Partial Throat Restriction and Impeller with Balance Holes.

The flow structure and average velocity in the enlarged cylindrical chamber with a partial throat restriction were very similar to those of the tapered chamber with the same size throat restriction. The four degree taper does not seem to have a significant effect on the flow structure although the total turbulence intensity in the four degree tapered chamber is somewhat less at 14 percent than is the cylindrical bore which measures 17 percent.

Seal chamber velocities were at a minimum with impellers having no balance holes or back pumpout vanes. Without these features, the volumetric flow through the chamber and the transfer of rotational energy to the fluid is minimized. As shown in Table 1, the flow velocities in seal chambers with impellers having no balance holes or back pumpout vanes were in the range of 6.6 to 13.1 ft/sec (2.0 to 4.0 m/s), while the same impellers with balance holes had velocities of 26.9 to 27.9 ft/sec (8.2 to 8.5 m/s).

Plugging the balance holes diminished the fluid exchange between the two sides of the impeller so that the chamber behaved as a closed tube. Previous experiments [7] have shown that for a closed tube with an inner rotating shaft, the flow velocity drops from the rotational speed of the shaft to zero at the chamber bore. Measured results were consistent with these previous findings. Field experience shows similar reductions in velocities in the seal chamber can be experienced by removing back pumpout vanes from the impeller. The removal of back pumpout vanes or the plugging of balance holes is not always an acceptable solution to controlling high velocities in the seal chamber. Pump manufacturers often utilize these impeller features to optimize the life of thrust bearings.

In the region near the corner of the gland face and the seal chamber bore, the axial and radial velocity components are not sufficient to overcome the centripetal force of the larger particles (>100 μm). Thus, the particles become entrapped, as shown in Figure 9. Small particles (<100 μm) are swept through the chamber

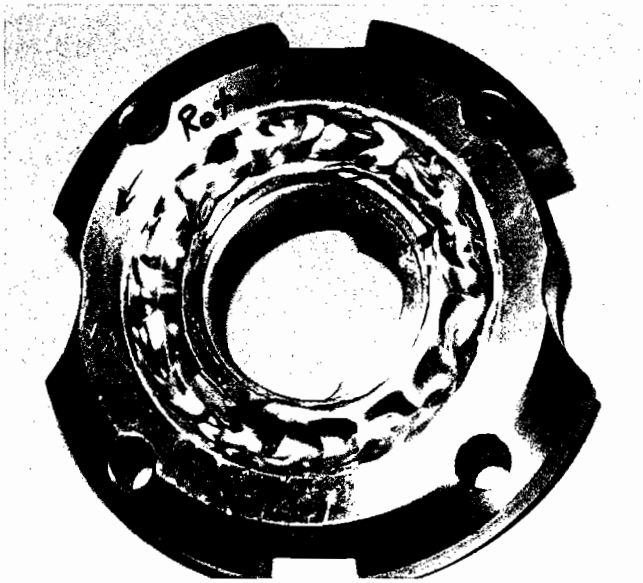

Figure 3. Typical Gland Erosion Pattern.

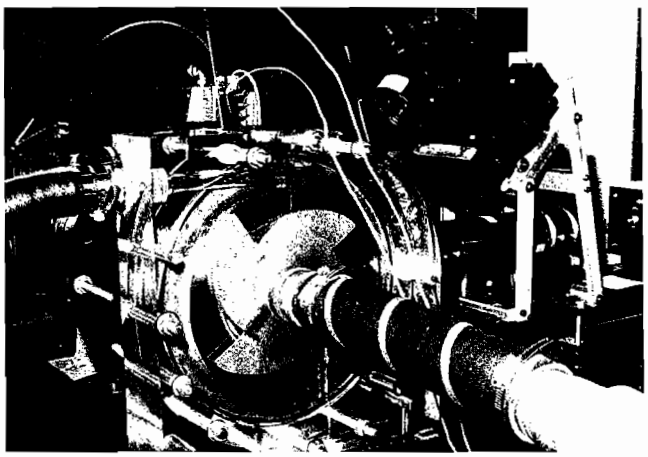

Figure 4. Acrylic Pump.

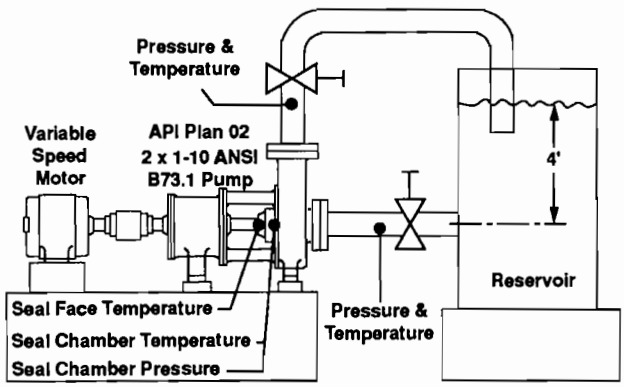

Figure 5. Flow Diagram of Acrylic Pump System.

Seal face temperatures were monitored and used as an indicator of seal face lubrication. Thermocouples were installed 0.06 in (1.5 mm) back from the stationary face and in the seal chamber near the gland face. Data on pressure and temperatures in the systems were recorded five times per second.

To measure and record the fluid flow in the seal chamber, the pumped fluid (water) was seeded with 9.0 micron silver-coated plastic particles having a specific gravity of 2.6. Flow visualization and LDV techniques were then used to track the flow path of the particles and to measure the velocity at various points in the seal chamber (Figure 6). The velocity and turbulence intensity measurements were made with a single component 100 MW argon-ion dual beam LDV system. Velocity and turbulence intensity components were measured individually using the back scattering technique. For flow visualization, a narrow sheet of laser light was generated by shining the laser beam on a cylindrical reflecting surface. The diverging reflected light was then passed through a cylindrical lens that converted the reflected light to parallel rays, thereby forming an intense sheet of light for selective visualization. The flow velocity information was fed into CFD programs to predict performance of existing and possible new seal chamber designs. These programs proved invaluable in the development of seal chamber modifications discussed later. Flow visualization was captured by high speed video at 1,000 frames per second using 40 to 700 micron particles. Additional temperature and vibration tests under cavitating conditions were conducted on an ANSI B73.1 pump as described later.

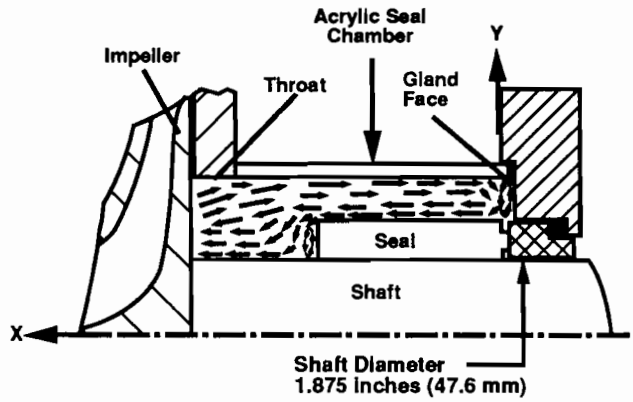

Figure 6. Typical Flow Pattern Analysis.

FLOW AND EROSION STUDIES

Test Results

In order to establish fluid flow maps for six sets of impeller and seal chamber combinations, LDV measurements were taken at 96 different points in the seal chamber. At each of these points, azimuthal, axial, and radial components of the velocity were measured. Flow velocities shown in Table 1 are an average value for the entire flow region in the chamber around the seal. Under all conditions, the major component of the velocity was in the azimuthal direction. The magnitudes of the velocity components in the axial and radial directions were approximately 10 percent of those in the azimuthal direction.

As the name implies, "turbulence intensity" is a nondimensional measure of the turbulence level in, for example, a seal chamber. In order to obtain the total turbulence intensity, the variances between the mean velocity at each location and the individual samples of axial, radial, and azimuthal velocities were determined. Next, the root-mean-square values of the variances were calculated and then divided by the reference seal surface linear speed of 19 ft/sec (5.8 m/s) to yield a turbulence intensity value. The values in Table 1, shown as a percentage of the reference speed, are the sum of the maximum magnitudes of turbulence intensity in the axial, radial, and azimuthal directions.

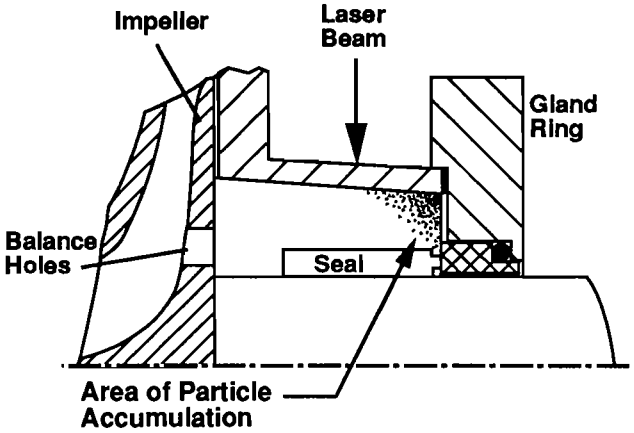

Figure 9. Accumulation of Large Particles in Enlarged Tapered Seal Chamber.

and do not become trapped as easily as the large particles. Indeed, the distribution of particles in the chamber and within the vortices is a function of their density and volume (i.e., mass).

As a result of the high azimuthal velocities and the accumulation of large particles, severe shear erosion can occur at the gland face and at the chamber bore near the gland face, as previously shown in Figure 3.

PREDICTION OF EROSION

The "abrasive power" equation generated by Bovet [8] has been used to predict erosion of various pump components. Bovet's Equation (1) as stated below describes the abrasive power of a slurry in terms of its kinetic energy.

$$P = \mu \frac{4\pi d^3}{3R} (\rho_d - \rho_f) U^3 \qquad (1)$$

where:

$(\rho_d = \rho_s C + \rho_f(1 - C)$

and: P = Abrasive power
μ = Coefficient of friction for particle - surface
d = Solid particle diameter
R = Radius of curvature of eroded material
ρ_s = Particle density
ρ_f = Fluid density
U = Average flow velocity
C = Volumetric transport concentration

The lack of accurate flow velocity, particle surface friction coefficients, and other data for a given field application limits the practical ability to directly utilize Bovet's Equation (1) as a tool to predict when erosion problems might be expected to occur in a given field application. However, while factors such as particle shape, hardness, angle of impingement, etc., are also important, it is possible to estimate the potential for seal chamber erosion without them by developing a new, simplified "erosion index" formula, as described below, and comparing the results with field case histories.

The key to predicting seal chamber erosion is to accurately estimate the velocity in the seal chamber which varies dramatically due to both seal chamber and impeller design. To accurately predict velocities, measurements were taken using LDV techniques to establish seal chamber design factors, F_c, shown in Table 2, for various pairs of impeller and seal chamber designs. F_c is

Table 2. Seal Chamber Design Factors.

Chamber Design	Throat	Impeller	Seal Chamber Design Factor, F_c
Standard	Restricted	All	0.3
Enlarged[1]	Open	Smooth[2]	0.7
		Balance Holes	1.9
		Pump Out Vanes	1.9
	Partially Restricted	Smooth[2]	0.4
		Balance Holes	1.1
		Pump Out Vanes	1.1
30 to 45° Flared	Open	Smooth[2]	0.9
		Balance Holes	1.9
		Pump Out Vanes	1.9

1. Cylindrical and 4 to 5° tapered bore.
2. Closed or semi-open impeller without balance holes or back pump-out vanes.

simply the measured velocity, divided by the shaft speed of 14.7 ft/sec (4.5 m/s). The average velocity is thereby estimated by multiplying the velocity of the O.D. of the shaft times F_c. When the velocity in the seal chamber is known, the erosion potential of any given application can be easily predicted. The information needed for the analysis includes:

ϕ = Shaft Diameter (inches)
N = Shaft Speed (revolutions per second]
F_c = Seal Chamber Design Factor (from Table 2)
D = Seal Chamber Bore (inches)
C = Solids Concentration (percent by volume)
S_S = Specific Gravity of the Solids
S_L = Specific Gravity of the Liquid
d = Maximum Particle Diameter (Microns, μm - reference Table 3)

This information is applied to the equations below which yield a relative Velocity Factor, F_v, Equation (2), and Solids Factor, F_s, Equation (3).

$$F_v = \frac{(\phi \times N \times F_c)^3}{D} \qquad (2)$$

$$F_s = C(S_S - S_L)d^3 \qquad (3)$$

These two factors are multiplied to yield an overall erosion index value (EIV), Equation (4).

$$EIV = F_v \times F_s \qquad (4)$$

In Figure 10, the calculated EIV is compared with actual field case histories. The data points are keyed to the examples in Table 4. From these comparisons, it is possible to project the range of potential erosion for any given application. The actual erosion experienced will vary somewhat, based on particle hardness, shape, etc.

Table 3. Approximate Size of Particles.

Substance	Size, microns
Clay	2
Talcum Powder	10
Lime	40
Table Salt	100
Fine Sand	200
Fly Ash	200
Milled Ore	100 - 1000
Diatomaceous Earth	110 - 700

Table 4. Test and Field Application Erosion Results.

Number	Shaft Diameter, Inches	RPM	Seal Chamber Design Factor	Percent Solids by Volume	Paricle Size, Microns	Particle Specific Gravity	Erosion Index Value EIV x 10^{12}	Erosion Rates Reported per Year
1	1.750	3480	1.9	20	110	2.3	71	0.5 in. (12.7 mm)
2	1.750	1725	1.9	20	110	2.3	9	0.06 in. (1.5 mm)
3	1.875	3480	1.1	20	110	2.3	16	0.3 in. (7.6 mm)
4	1.875	1725	1.1	20	110	2.3	2	Nil
5	1.500	3600	1.9	10	100	6.0	86	> 0.5 in. (12.7 mm)
6	1.875	3600	1.9	5	100	4.0	41	> 0.5 in. (12.7 mm)
7	2.290	1200	1.1	20	108	6.0	3	Nil
8	1.875	1700	1.9	0.5	500	2.6	25	> 0.5 in. (12.7 mm)
9	1.875	3535	1.9	0.5	400	2.6	132	> 0.5 in. (12.7 mm)
10	1.375	3600	1.9	0.5	180	2.3	6	0.03 in. (0.8 mm)
11	3.970	700	0.7	25	850	6.0	307	> 0.5 in. (12.7 mm)
12	3.970	700	0.7	20	300	6.0	11	0.06 in. (1.5 mm)
13	3.970	1250	0.7	30	385	6.0	171	> 0.5 in. (12.7 mm)

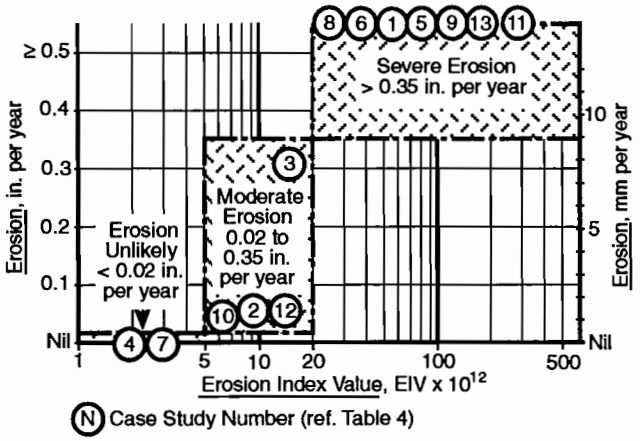

Figure 10. Erosion Index Value Vs Actual Erosion.

If a calculation indicates that there is a high potential for erosion in a new application, steps may be taken to reduce that possibility. From a practical perspective, it is unlikely that the product concentration, specific gravity, or particle diameter can be altered. However, a new pump may be selected and sized to minimize the velocity factor (F_v). Note that the values for shaft diameter (ϕ), shaft speed (N), and seal chamber design factor (F_c) are raised to the third power in calculating F_v. Also, the maximum seal chamber bore (D) may be selected. Seal chamber and impeller designs may be chosen to minimize F_c. As an example, an impeller with back pumpout vanes has an F_c of 1.9 when it is used with an open enlarged seal chamber (Table 2). By substituting an impeller having a smooth back, that is with no back pumpout vanes or balance holes, F_c is reduced to 0.7. Since F_c is a cubed variable, F_v is reduced by a factor of 20.0 (Equation (2)). In actual mining services, such a change to large slurry pumps improved seal life from one to two months to one to three years.

To correct an erosion problem in an existing installation, the most practical approach may be to replace or modify the seal chamber with a design that will minimize F_v. Wear resistant chamber bore and gland materials can also be installed. Occasionally, an external flush is added to reduce the solids concentration in the seal chamber and thereby reduce erosion.

CASE STUDIES

• A 2 × 1-10 ANSI B73.1 pump operating at 3480 rpm and handling 20 percent diatomaceous earth was experiencing 0.013 in (0.3 mm)/day of gland plate erosion. The pump, equipped with an open five degree tapered chamber, was found to have an EIV of 71 × 10^{12}. From Figure 10, it is obvious that severe erosion would be expected. To reduce erosion, a cylindrical bore seal chamber having a partial throat restriction was installed in place of the five degree tapered chamber. This change reduced the seal chamber design factor, Fc, from 1.9 to 1.1 and the subsequent EIV from 71 × 10^{12} to 14 × 10^{12}. This change reduced measured 316 SS gland plate erosion from 0.013 in (0.3 mm)/day to 0.0008 in (0.02 mm)/day. See Studies 1 and 1A in Table 5 for details.

Table 5. Erosion Case Studies.

Number	Shaft Diameter, Inches	RPM	Seal Chamber Design Factor	Percent Solids by Volume	Particle Size, Microns	Particle Specific Gravity	Erosion Index Value, EIV x 10^{12}	Observations
1	1.750	3600	1.9	20	110	2.3	71	Erosion rate=0.013 in./day (0.3 mm/day)
1A	1.750	3600	1.1	20	110	2.3	14	Erosion rate=0.0008 in./day (0.02 mm/day)
2	3.970	700	1.9	20	300	6.0	211	Erosion failuras in 2-3 months
2A	3.970	700	0.7	20	300	6.0	11	Seal life 2-3 years

• A slurry pump operating in a mining service was failing from seal adapter plate erosion every one to two months. The pump, equipped with back pumpout vanes, was found to have an EIV of 211 × 10^{12}. By replacing the impeller with a "smooth disk" impeller, the EIV dropped to 11 × 10^{12} and the seal adapter life improved to two to three years. See Table 5, Studies 2 and 2A for details.

PROTRUSIONS REDUCE PARTICLE VELOCITIES, TURBULENCE, AND EROSION

Analysis

As stated previously, the axial and radial velocity components at the gland and chamber bore corner are not sufficient to overcome centripetal force of larger particles. As a result of the azimuthal velocities and the accumulation of large particles, severe shear erosion can occur in this region.

It was determined that some form of rib, strake, or protrusion extending axially along the chamber wall could reduce the high azimuthal velocity and impart an inward radial velocity to the particles, Figure 11. This change in velocity and direction would then allow the particles to exit the chamber with the outflow.

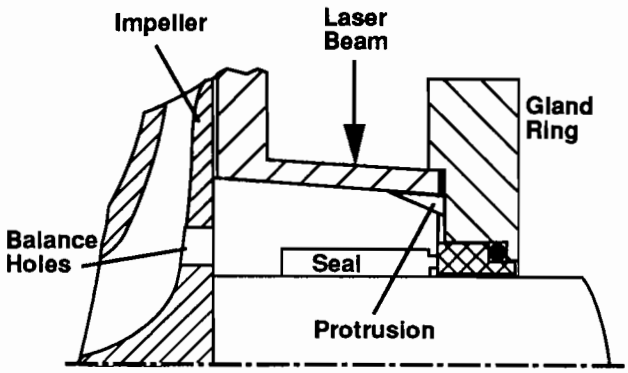

Figure 11. Protrusions in Enlarged Seal Chamber.

Through the use of computational fluid dynamics (CFD), these phenomena were accurately modeled using the LDV measured seal chamber throat velocity data as the inlet boundary conditions. Through further use of CFD, several sets of protrusions were developed and then tested. In all tests, four protrusions were equally spaced around the seal chamber bore. The typical configuration of the protrusions tested is shown in Figure 12.

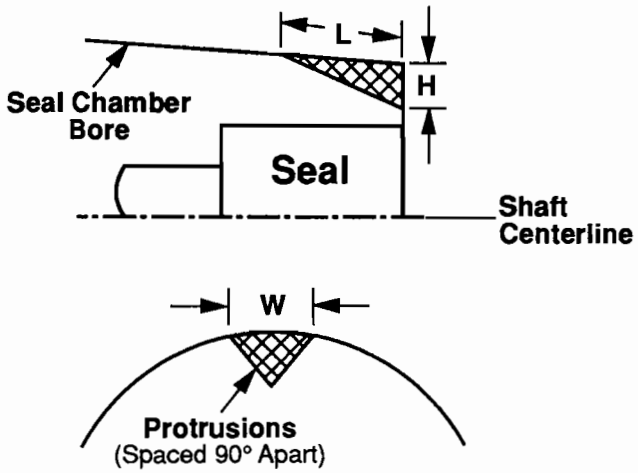

Figure 12. Typical Protrusion Arrangement.

Test Results

The accumulation of solids near the gland face was significantly reduced by all protrusion designs. In addition, the protrusion set having the greatest height significantly reduced the solids concentration in the seal chamber. LDV measurements revealed that the addition of this protrusion set also reduced the azimuthal velocity components by up to 50 percent, while increasing the radial velocity towards the shaft by as much as 400 percent.

ENTRAINED GASES AND AIR INGESTION

The ability to pump liquid and gas mixtures is vital to many industrial processes. Such applications range from water to a variety of slurries with entrained gases such as in flue gas desulfurization systems and paper stock.

Because the seal chamber is a low pressure point in the system and temperatures are normally high relative to the entire system, gases are able to come out of solution or suspension and accumulate in the seal chamber at the seal faces, where they are least desirable. Other means of air ingestion or vaporization include a variety of off-design pumping conditions as listed below. This research demonstrates that certain seal chamber designs are more prone to gas accumulation problems than others. Thus, the seal chamber design and selection can play a significant role in minimizing seal-related performance problems from fluids with entrained gases or off-design operating conditions.

Sources of air ingestion, entrained gas, vaporization, and gas accumulation include:

- Gases that come out of solution in chamber because it is a low pressure point in the system.
- Operating beyond the pump curve best efficiency point (BEP).
- Operating the pump too far back on the pump curve.
- Cavitation conditions.
- Inadequate net positive suction head (NPSH).
- Formation of vortices in tanks and at pump suctions.
- Leaking valves and gaskets.
- Excessive temperature rise in chamber, especially with low boiling point margin (BPM) fluids.
- Vacuum conditions in the chamber.
- Paper stock and other fibers containing entrained air.
- Entrained gases in slurries.

Off-Design Pump Operation

Pump components, i.e., shaft, impeller, casing, bearings, etc., and piping are designed to operate at the pump's BEP as determined from the published pump curve. The pump is generally considered to be pumping "off the curve" if it is required to pump 20 percent more or 60 percent less than its BEP.

Various publications relate equipment operation to MTBPM [9]. Shiels [10] also points out some of the specific problems that are caused by off-design pump operation. These include:

- High internal temperature rises.
- Flashing of the product.
- Low flow recirculation damage.
- Reduced bearing and seal life due to shaft deflection.
- Suction recirculation.
- Cavitation.
- Shaft deflection.

Various detrimental effects due to operating a pump off of its BEP are shown in Figure 13. Short bearing and seal life occur long before traditional danger signs such as cavitation and excessive temperature rise occur.

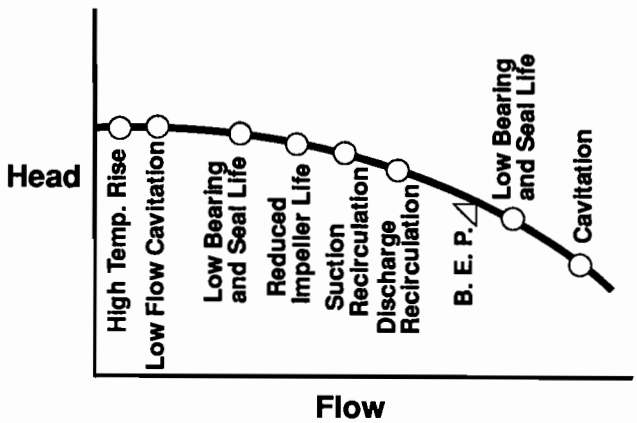

Figure 13. Effects of Operating a Pump Off its Best Efficiency Point (BEP).

To more accurately measure the effects of off-design pump operation on seal life and emissions, an overhung centrifugal pump was set up under laboratory conditions to operate at 3600 rpm with a 1.75 in metal bellows seal while purposely restricting the flow below the pump's recommended window of operation until pump cavitation occurred.

To monitor the effects of these abnormal conditions on seal performance, a pump was fully equipped with pressure, temperature, and vibration monitoring probes (Figure 14). Two noncontacting 8.0 mm proximity probes were mounted 90 degrees apart over the seal chamber gland and spaced 0.050 in (1.27 mm) from the face end of the bellows. Two 5.0 mm proximity probes were also mounted next to the gland to measure shaft sleeve deflection on the atmospheric side of the seal. One 5.0 mm proximity probe was mounted over the coupling keyway to measure motor rpm.

The feasibility of measuring axial bellows displacement was investigated, but due to the configuration of the bellows design, this was not performed because of modifications required to the bellows end piece. It was decided that adding mass to the end piece would lower the natural frequency of the bellows system and obstruct proper studies.

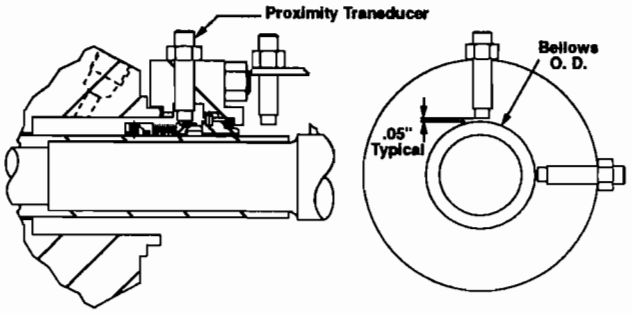

Figure 14. Off-Design Pump Cavitation Test Unit.

The seal face temperature was again monitored with a thermocouple mounted 0.06 in (1.52 mm) back from the stationary seal face. The seal chamber temperature was monitored with a thermocouple located 0.25 in (6.25 mm) from the seal faces. During normal pump operation, both the shaft sleeve and bellows seal face end piece had peak-to-peak vibrations of less than 2.0 mils (0.05 mm). Under pump cavitation modes, shaft sleeve displacement increased from 1.9 to 8.4 mils (0.05 to 0.21 mm). Bellows end piece/seal face vibration was measured at 13 to 35 mils (0.33 to 0.89 mm).

The seal chamber pressure was measured at a slight vacuum under these test conditions. Long term testing from 24 to 43 hours showed seal face temperature excursions from 330°F to 800°F (166°C to 300°C) over pump product temperature (Table 6). Observations showed excessive seal face temperature excursions were being caused by constant drawing of gases across the seal faces and the formation of a gas bubble inside the seal chamber near the seal faces during pump cavitation. It was interesting to tear down and inspect the seal after these 24 to 43 hour periods of off-design operation. The seal faces showed only slight signs of chipping on the I.D. and the O.D., and the O-ring secondary seals were surprisingly only slightly squared up from excessive seal face temperatures. This was significant since many of the failures returned from the field frequently show O-rings burned or melted, indicating that even higher seal face temperatures and longer periods of dry running sometimes occur.

Table 6. Effects of Pump Cavitation on Seal Performance.

	Normal Pump Operation	Pump Cavitation Mode
Seal Chamber Temperature, F	150	150
C	65	65
Shaft Sleeve Vibration, mils p-p	1.9	2 to 8.4
Seal Face Vibration, mils p-p	< 2.0	13 to 35
Seal Face Temperature, F	152 to 165	330 to 800
C	67 to 74	166 to 427

Dry Running Conditions

The preceding findings of seal damage may be typical of many sealing applications where seal chambers operate under negative pressures or the process fluid contains entrained gases that come out of solution in the seal chamber due to low pressure or due to the temperature rise that normally occurs.

Computational fluid dynamic (CFD) modelling and flow visualization studies indicate one way of protecting the seal is to create a localized higher pressure around the seal in the seal chamber. Higher pressure may protect the seal from gases and resulting loss of face lubrication by sweeping the entrained gases away from the seal faces and maintaining a liquid film at the seal faces. New seal chamber designs to automatically compensate for entrained gas and dry running conditions are under study.

With the aid of high speed (1000 frames/sec) videography, the flow of fluid, solids, and air was observed in various seal chambers under off-design conditions. These conditions included operating the pump with the discharge valve restricted, cavitation conditions, and vacuum conditions to -14 psig (-97 kPa) in the seal chamber. Both four degree tapered and 30 degree flared chambers were tested, with a variety of impeller designs. The initial results are summarized in Table 7.

Table 7. Off-Design Performance Comparisons.

Suction Pressure psig (kPa)	Discharge Pressure psig (kPa)	Chamber Pressure psig (kPa)	Seal Chamber Design	Impeller Design	ΔT Seal Face vs. Chamber F (C)	Air Ingested	Air Trapped	Degree of Solids Accum.
-0.2 (-1.4) (normal)	26.6 (183)	-0.8 (-6)	4° Tapered	Balance Holes	4(2)[1]	No	No	High
-13.5 (-93) (restricted)	17.0 (117)	-13.7 (-94)	4° Tapered	Balance Holes	31 (17)[2]	Yes	No	High
0.0 (0.0) (normal)	24.0 (166)	-2.0 (-13.7)	4° Tapered	Vanes	11 (6)[1]	No	No	Moderate
-13.0 (-90) (restricted)	10.2 (70)	-14.0 (-97)	4° Tapered	Vanes	61 (34)[2]	Yes	Yes	Moderate
-1.0 (-6.9) (normal)	25.0 (179)	10.0 (69)	30° Flared	Smooth (no bal. holes)	11 (6)[1]	No	No	Moderate
-14.0 (-97) (restricted)	10.0 (69)	-14.0 (-97)	30° Flared	Smooth (no bal. holes)	54 (30)[2]	Yes	Yes	Moderate
0.0 (0.0) (normal)	24.0 (166)	2.0 (13.7)	30° Flared	Balance Holes	13 (7)[1]	No	No	Moderate
-14.0 (-97) (restricted)	10.0 (69)	-14.0 (-97)	30° Flared	Balance Holes	43 (24)[2]	Yes	No	Moderate

Note 1, steady state.
Note 2, temperature rise in ten seconds.
All tests at 1750 rpm with 1.875" welded metal bellows and face mechanical seal.

The initial data provide further evidence that seal chamber configuration and impeller design have a measurable impact on flow in the seal chamber and the resulting ingestion of air.

Significant findings from these tests include the following:

- Vacuum conditions can exist in the chamber under otherwise normal pump operating conditions.
- Seal face temperatures increase almost immediately under vacuum-induced dry-running conditions, but the actual temperature rise and rate of temperature rise vary with the type of impeller and seal chamber design.
- Impellers with balance holes generate higher flow velocities than smooth impellers, but also evacuate any ingested air or gas bubbles created in the chamber during high vacuum conditions once the pump returns to normal operation.
- Smooth and vaned impeller designs tend to trap the air behind the impeller once the air is drawn into the chamber.
- High flow through the chamber reduces gas accumulation while the use of throat restrictions increase the possibility of gas entrapment.
- Open throat tapered and flared chambers vent gas upon shutdown.

Not all possible combinations of seal chamber configurations and impeller designs have been tested to date and further research is needed to more accurately quantify impeller design effects on gas ingestion.

SEAL CHAMBER SELECTION GUIDELINES

Based on the preceding observations and analysis, it is concluded that selecting the proper seal chamber designs and environmental controls for various applications can significantly extend

MTBPM. To aid in this selection process, Tables 8 and 9 were developed. Seal chamber preference for various environmental conditions are rated in Table 8. As an example, if the application is known to contain entrained gases, the preferred seal chamber of existing commercial technology is the four to five degree tapered seal chamber. This is rated over the other seal chambers because of its self-venting feature under start-stop conditions and the typically higher pressure developed in the seal chamber under normal operation. Both of these factors should enhance seal face cooling and seal face lubrication, thus improving seal life. Various pump environmental conditions, as shown in Table 9, may exist with the six most common, commercially available seal chambers and the environmental controls that should be used with each seal chamber to optimize seal life are also identified. As an example, if solids are present at a concentration greater than ten percent by volume, the conventional seal chamber would require an external flush or double mechanical seal. A four to five degree tapered seal chamber would be preferred for its ability to resist packing with solids and to readily transfer heat away from the seal faces. To preclude damage from erosion, the EIV should be calculated and minimized as previously described.

Table 8. Selection of Optimum Seal Chamber Under Various Conditions.

Seal Chamber ►	Conventional Stuffing Box	4 - 5° Tapered Bore Enlarged Chamber	Cylindrical Enlarged Chamber	Cylindrical Bore Enlarged Chamber Partial Throat Restriction	Cylindrical Bore Enlarged Chamber Throat Restriction	30° Flared Enlarged Chamber
Configuration ► / Application Environment ▼						
Maximum Heat Transfer with Pump Product	4	1	1	2	3	1
Eliminate Gas in Seal Chamber Under Start / Stop Conditions	4	1	2	3	4	1
Best Able to Handle Low BPM Fluids	4	1	2	2	3	1
Best for Slurries	4	1*	2*	2	3	1*

1 = optimum choice , 4 = less optimum choice

* Calculate EIV and minimize to avoid erosion

Table 9. Environmental Recommendations for Various Seal Chambers and Conditions.

Seal Chamber ►	Conventional Stuffing Box	4 - 5° Tapered Bore Enlarged Chamber	Cylindrical Enlarged Chamber	Cylindrical Bore Enlarged Chamber Partial Throat Restriction	Cylindrical Bore Enlarged Chamber Throat Restriction	30° Flared Enlarged Chamber
Configuration ► / Condition ▼						
• No gas or vapor likely • Solids <10% by volume	Bypass or external flush	No flush required Erosion possible Minimize EIV	No flush required Erosion possible Minimize EIV	No flush required	Bypass or external flush	No flush required Erosion possible Minimize EIV
• Gas ingestion likely • Solids <10% by volume	Bypass or external flush	No flush required Quench recommended Erosion possible Minimize EIV	No flush required Quench recommended Erosion possible Minimize EIV	No flush required Quench recommended	Bypass or external flush	No flush required Quench recommended Erosion possible Minimize EIV
• Light HC or other low BP fluid • Chamber within 25 psig of BP	Bypass flush with throat bushing	Not recommended	Not recommended	Bypass flush with throat bushing	Bypass flush with throat bushing	Not recommended
• Chamber >25 psig of BP	Bypass flush	No flush required	No flush required	No flush required	Bypass flush	No flush required
• Solids >10% by volume	External flush or double seal	No flush required Erosion possible Minimize EIV	No flush required Erosion possible Minimize EIV	No flush required	External flush or double seal	No flush required Erosion possible Minimize EIV
• Gas ingestion likely • No solids	Bypass flush	No flush required	No flush required	No flush required	Bypass flush	No flush required

Bypass Flush — API Piping Plan 11, External Flush — API Piping Plan 32, No Flush — API Plan 02, Double Seal — API Piping Plan 53

CONCLUSIONS

In an industry-wide effort to improve the uptime of centrifugal pumps, pump and seal standards have been updated to include enlarged-bore, seal-only chambers as options to the conventional packed stuffing box. Studies demonstrate that fluid flow within the enlarged-bore chambers is increased, which supports the following conclusions:

- Open enlarged seal chambers enhance the removal of seal-generated heat.
- The concentration of large, high-velocity particles at the corner of the gland face and chamber bore can result in excessive localized erosion. Minimizing erosion index values (EIV) can help to avoid these erosion problems and still enhance other positive enlarged-bore seal chamber attributes.
- Negative seal chamber pressure via cavitation, etc., can seriously shorten seal life. Selecting the proper combination of impeller and seal chamber can reduce these effects.
- The future development of appropriately configured strakes and protrusions may be an effective method of reducing the accumulation of solids and gases in the seal chamber.
- Further research is still needed to observe and quantify fluid and solid particle flows in applications such as lime slurries where the use of a flush may still be the preferred approach.

The work completed to date, based on current studies of flow paths and velocities in the seal chamber, has resulted in application guides that can be used to optimize mechanical seal life.

REFERENCES

1. Barnes, N.D., Flitney, R.K., Nau, B.S., "Considerations Affecting the Design of Pump Chambers for Improved Mechanical Seal Reliability," BPMA 12th International Pump Technical Conference (1991).
2. ASME Standard B73.1M, "Specification for Horizontal End Suction Centrifugal Pumps for Chemical Process," The American Society of Mechanical Engineers, New York, NY (1991).
3. API Standard 610, Seventh Edition, "Centrifugal Pumps for General Refinery Services," American Petroleum Institute, Washington, D.C. (1989).
4. DIN 24 960, "Mechanical Seals: Cavities, Principal Dimensions, Designation and Material Codes," Normenausschuß Maschinenbau (NAM) im DIN Deutsches Institut für Normung e.V. (1990).
5. ISO 3069, "End Suction Centrifugal Pumps—Dimensions of Cavities for Mechanical Seals and for Soft Packing," (1974), Proposed Revision (1992), International Standards Organization.
6. Davison, M., "The Effects of Seal Chamber Design on Seal Performance," Proceedings of the Sixth International Pump Users Symposium, Turbomachinery Laboratory, Department of Mechanical Engineering, Texas A&M University, College Station, Texas (1989).
7. Polkowski, J. S., "Turbulent Flow Between Coaxial Cylinders with the Inner Cylinder Rotating," Transactions of the ASME, *106* (1984).
8. Bovet, T., "Contribution to the Study of the Phenomenon of Abrasive Erosion in the Realm of Hydraulic Turbines," Bulletin Technical Science Romeanda, 328-337, *8493* (1958).
9. Flitney, R. K. and Nau, B. S., "Reliability of Mechanical Seals in Centrifugal Process Pumps," BHRA International Fluid Sealing Conference, Paper A2, Cannes, France (1986).
10. Shiels, S. T., "Centrifugal Pump Specification and Selection—A System's Approach," Fifth International Pump Users Symposium, Turbomachinery Laboratory, Department of Mechanical Engineering, Texas A&M University, College Station, Texas pp. 93-107 (1989).

ACKNOWLEDGMENTS

The authors wish to thank the National Science Foundation, Dr. Parviz Merati, and Mr. Joseph Parker, Western Michigan University, for their support and interest in this work.